SAND2018-7243C

Characterization of Hypervelocity Fragments and Subsequent HE Initiation

Daniel R. Guildenbecher[*], Joseph D. Olles[*], Timothy J. Miller[*], Phillip L. Reu[*], John D. Yeager[#], Patrick D. Bowden[#] and Andrew M. Schmalzer[#]

[*]Explosive Operations Center of Excellence
Sandia National Laboratories, Albuquerque, New Mexico, USA

[#]High Explosives Science and Technology
Los Alamos National Laboratory, Los Alamos, New Mexico, USA

Abstract. Several common detonators involve high explosive drivers and metal end-caps or cups. Upon initiation these break apart into a cluster of metal fragments traveling at hypersonic velocities. This work leverages modern MHz rate cameras for experimental investigation of this fragmentation process and the potential for subsequent initiation of other high-explosives upon impact. When recorded at 5 million frames-per-second, stereo Digital Image Correlation (DIC) is shown to provide detailed resolution of the initial 3D metal strain. The size and velocity of the resulting fragments are subsequently measured at 2 million frames-per-second using custom tracking algorithms introduced here.

Introduction

Much work has been done to interrogate plastic-bonded explosives (PBX) related to run-distance-to-detonation as a function of well-characterized input stress (Pop plot)[1] and critical diameter/spot size[2]. However, in off-normal situations, such as single or multiple fragment impact, it is more difficult to assess PBX initiability[3, 4]. Here we study standoff firing of a detonator, which launches fragments that are neither spherical nor planar. Fig. 1 shows select images from a high-speed video of this event.

Fragmentation of metal cased explosives and initiation of PBX by fragment impact are both stochastic processes. Consequently, it is inevitable that chance (or statistics) plays a role in whether a specific experiment causes PBX initiation. Because of this, it is impossible to experimentally study all relevant conditions. Rather, we aim to investigate select conditions so that data can be applied for development of models appropriate for investigating a more complete suite of parameters.

Previously, we applied Digital Inline Holography (DIH) to quantify the initial fragment size and velocity in the experiment shown in Fig. 1[5]. As discussed further in this work, this method has specific advantages and drawbacks for application to hypervelocity fragments. Here, we propose additional diagnostics for more complete characterization of these fragments. In addition, methods are proposed for detailed investigation of fragment formation via quantification of the explosively driven strain of the detonator case.

This work is enabled by significant recent advancement in high-speed imaging, specifically modern MHz rate cameras[6] enable video imaging of this process with temporal resolution that was previously impossible or much more difficult.

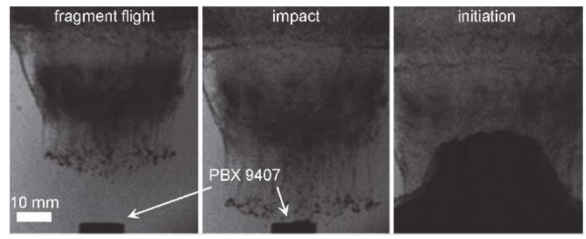

Fig. 1. Fragment impact and initiation of PBX.

The remainder of this paper begins with a brief review of our previous work. Next, 5 MHz stereo Digital Image Correlation (DIC) is shown to quantify the 3D strain field of the detonator prior to fragmentation. At increased standoff, a similar configuration is shown to allow 3D quantification of the fragment field. Finally, initial application of these techniques to PBX initiation is demonstrated.

Previous Work

Many research groups have previously focused on quantification of explosively driven metal fragmentation and fragment impact. In lieu of a complete review, we focus here on only our own recent work to provide context for the new results shown in the subsequent sections.

The size and velocity of fragments produced by a metal cased explosive is strongly related to the initial strain rate of the case. Digital Image Correlation (DIC) is an imaging method for full-field surface strain which has been widely applied to study solid mechanics[7-9]. The technique is based on tracking the motion of a speckled surface over time. With two cameras in a stereo configuration, triangulation can be used to find the 3D surface motion. In 2010, the best high-speed cameras were capable of a maximum of ~1 MHz record speeds. With that, we were able to use DIC to quantify the explosively loaded strain of ~10 cm diameter hollow metal hemispheres loaded with 300 g of explosives.[7] Here, we are interested in the fragmentation of detonators with explosive loading on the order of ~1 g and dimensions on the order of ~10 mm. Assuming similar velocities, the smaller required field-of-view (FOV) in the current detonator experiments necessitates faster record rates for similar resolution of temporal dynamics. As shown here, with the very recent advancement of ultra-high-speed cameras to 5 MHz, these experiments are finally feasible.

Measurement of size and velocity of fragments can be performed in many ways. For lab-scale experiments, such as the detonator scales studied here, we recently proposed Digital Inline Holography (DIH).[5] The experimental setup is shown in Fig. 2. A coherent and collimated laser beam is propagated through a particle field resulting in the formation of diffraction patterns which are imaged with a camera. An example raw hologram image for fragments traveling from bottom to top is shown in the left-hand side of Fig. 3. This image is numerically refocused by modeling each pixel as the source of a spherical wave which convolve at a refocus plane according to the Huygens–Fresnel principle.[10] By searching for the optical depth where each particle is in best focus, the 3D location and 2D refocused morphologies can be quantified as shown in the right-hand side of Fig. 3. Multiple holograms recoded with short inter-frame time allow for measurement of fragment velocities.

In Yeager *et al.*[5] DIH was applied to measure the size and velocity of fragments produced by the same generic detonator studied in the PBX impact experiments shown in Fig. 1. This was used to provide a measured estimate of the impact conditions leading a go/no-go initiation transition.

As is clear in Fig. 3, DIH is also susceptible to image degradation due to index of refraction gradients, which in this case originate from gas-phase shock waves surrounding each hyper-velocity particle. To overcome this, Guildenbecher *et al.*[11] proposes a Phase Conjugate Digital Inline Holography (PCDIH) configuration. This utilizes 4-wave mixing to generate a backward propagating phase conjugate signal which largely removes the effects of shock waves after double passing the particle field as shown in Fig. 4. Although these results are promising for detailed 3D study of fragmentation, additional work is needed to extend this technique for temporal resolution using multi-pulse lasers similar to the traditional DIH work shown in Fig. 2 and Fig. 3. This is ongoing and largely requires acquisition of a multi-pulse laser system with sufficient coherence for wave mixing.

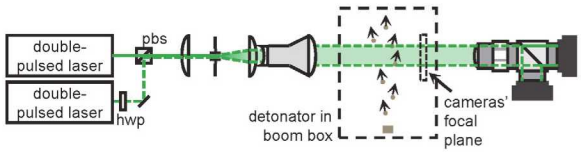

Fig. 2. Four-frame Digital Inline Holography (DIH) configuration (pbs: polarizing beam splitter, hwp: half-wave plate)[5].

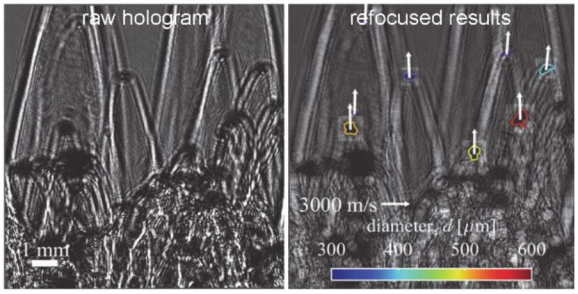

Fig. 3. Typical experimental results using the DIH configuration in Fig. 2[5].

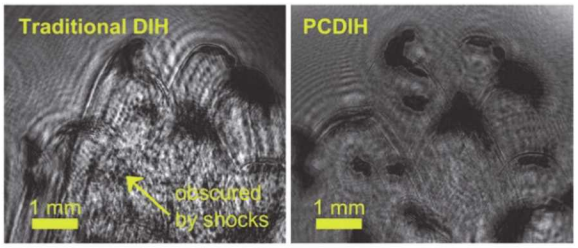

Fig. 4. Phase conjugate digital inline holography (PCDIH) reduces distortions due to shock-waves[11]

In the current work, alternative fragment tracking and sizing techniques are proposed which employ stereo imaging to obtain 3D information. Once again, the availability of cameras operating above 1 MHz are a critical enabling technology.

Digital Image Correlation (DIC)

The techniques demonstrated in this and the following section are applied to study the initial strain and fragmentation of a commercially available RP-80 detonator from Teledyne RISI. This explosive bridge wire initiated detonator contains 80 mg of PETN and 123 mg of RDX. This is incased by a cylindrical brass sleeve and an aluminum cup. Further details are available from Teledyne RISI.

Fig. 5 shows select frames from a high-speed video of the firing of an RP-80. At early times an aluminum flyer is produced which propagates upward in this video. Following this, the brass sleeve breaks apart to form a thick ring of fragments as shown in the right-most image of Fig. 5. In normal operations, the aluminum flyer is used to initiate a larger quantity of secondary explosive. Therefore, most previous work has focused on quantifying this flyer. Here, we utilize the RP-80 as a cost-effective test platform for fragmentation diagnostics. Therefore, the work discussed here focuses on the initial strain and fragmentation of the cylindrical portion of the case.

Strain is quantified using Digital Image Correlation (DIC), which is a full-field optical technique that uses stereo-camera pairs to measure the position, deformation, velocity and strain of surfaces. The rich data sets available from DIC are useful for validating the case behavior modeled by finite element simulations (FE). Metrics such as case deformation, velocity and strain provide diagnostic clues as to possible problems with the simulations. The early time behavior may also provide clues as to the later time fragments observed optically. A series of proof-of-concept DIC studies were conducted to determine optimum camera setup, lighting and DIC patterning techniques. Five tests, were conducted, with two different RP-80 geometries.

The DIC stereo-cameras were located behind protective view-ports approximately 20 cm away from the detonator. 105-mm Nikon Macro lenses imaged the detonator (Fig. 6) using two Shimadzu HPVX2 ultra-high-speed cameras. The FOV was approximately 22 mm × 13.4 mm, corresponding to the camera resolution of 400×250 pixels[2], with an approximate magnification of 18.4 pixels/mm. This allowed the entire detonator, outside the mount, to be viewed by the cameras. As this was a development project, some camera parameters were varied during the test series to find an optimum setup. For example, the first setup did not use scheimpflug mounts to align the detonator axis with the image plane and suffered from depth-of-field problems. The second setup that used the scheimpflug mounts had improved depth-of-field, but because of the different back focal length the sample was slightly closer to the cameras.

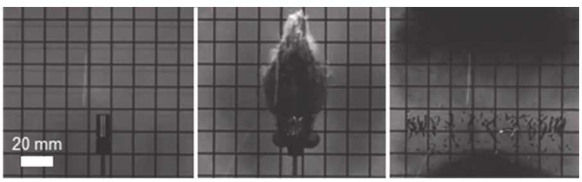

Fig. 5. Firing of an RP80 detonator. Images courtesy A. Baca, Sandia National Laboratories.

The Shimadzu camera was run at 5,000,000 frames-per-second and 200 ns exposure. Lighting was provided by 2 or 3 Silux 640 laser illumination systems. These pulsed lasers output at 640 nm wavelength with a bandwidth of 10 nm. When coupled with a liquid light guide, the lasers produced bright emission which is sufficiently incoherent such that laser speckle is not observed. Cross-polarizers were used on the lights and cameras to remove any glare from specular reflections off the surface. Bandpass filters were also used to attenuate most of the light created by the explosives. Because of the high-magnification, bandpass filtering, smaller apertures for increased depth-of-field, and cross-polarization, a large quantity of light was needed, making the pulsed Silux laser ideal for this application. Example images are shown in Fig. 6 illustrating the good image quality and excellent contrast of approximately 100 counts between white and black.

Speckling of the sample was done using a self-etching flat white spray paint (SEM 42043). This was applied the day of the test to ensure that the paint remained compliant[12]. Even with this precaution, there is evidence of paint failure during the experiment. Additional research will be required to determine the effects of this on the results and to develop mitigation. The black speckles were applied via a flat rubber stamp with 0.33 mm pads to create dots with diameters of between 3 and 8 pixels. A typical experiment, had an average speckle size of ~5 pixels and a 40% coverage.

The DIC analysis was done using Correlated Solutions, Inc. Vic3D software (v. 8.0.5) with example results shown in Fig. 7. The Variable Ray Origin (VRO) camera model was used to compensate for the viewport. Extended noise floor measurements were done by translating a flat plate throughout the measurement volume. Uncertainty estimates are based on these results. The DIC software settings for the analysis are shown in Table 1. Note that the data was correlated using incremental correlation due to the evolution of the strain surface during failure. The larger subset used for the first experiments was due to larger than desired speckle sizes. A virtual strain gage (VSG) size study was conducted and showed that the displacement and strain gradients are adequately captured.

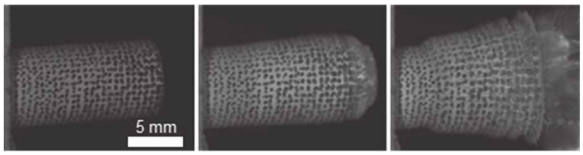

Fig. 6. Raw Digital Image Correlation (DIC) images of an RP-80 detonator recorded at 5 MHz.

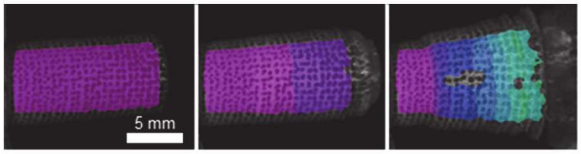

Fig. 7. DIC results colored by radial displacement.

Table 1. DIC Software settings.

DIC setting	Value
Subset size	19 × 19 pixels^2 or 29 × 29 pixels^2
Step size	1-pixel
Interpolant	8-Tap
Incremental correlation	Yes
Image filtering	Low-pass
Shape function	Affine
Strain window	5 data points

A cylindrical coordinate system was created by fitting a cylindrical surface to the initial measure surface and defining the detonator tip as $z = 0$ mm. The coordinate system is shown in Fig. 8. Cylindrical coordinates allow for a measurement of change in radius (dR) which is an important parameter of interest for model validation.

Timing and triggering was maintained during all the tests to allow for comparison between experiments. First motion was observed via DIC to occur at the same frame for all experiments with the standard RP-80 case design. One test was also performed on a modified RP-80 without the aluminum cup. It is assumed that the timing is the same as the previous tests with the same setup.

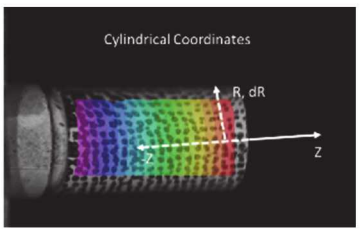

Fig. 8. Cylindrical coordinates used for all results

These results will be useful for model validation and investigations of the behavior of different geometry effects. For example, Fig. 9 shows the change in radius of the detonator at a select instant in time for five different tests. The four colored lines correspond to experiments using the typical RP-80 configuration as previously described. The noted grey line is from one test conducted using an RP-80 without the aluminum cup. Clearly, DIC can resolve the effects of the change in geometry.

DIC provides a robust method of getting material failure from the RP-80 case at meaningful frame rates and with acceptable uncertainties. Improvements in the future include: Improved painting techniques to mitigate paint failure and improved lighting. Furthermore, the simple RP-80 design, and our ability to manufacture this with different case materials and designs provides a cost-effective experimental design for validating a wide range of FE models.

Stereo Fragment Tracking

Fragment tracking and sizing is performed using a stereo image configuration nearly identical to the DIC setup discussed in the previous section. Here, the laser diode illuminators are rearranged to backlight the scene with the aid of a Plexiglas diffuser. The top row of Fig. 10 shows a few select images from one of the two cameras. In this case, a RP-80 detonator was placed approximately 75 mm above the FOV and oriented horizontally such that the camera views the downward propagation of the heavy ring of fragments produced by breakup of the cylindrical portion of the case. (Note: in the experimental images shown here, attempts were also made to collect the fragments into ballistic gel, resulting in the impact craters observed in the bottom of the images. Unfortunately, initial analysis of the collected fragments indicated a high likelihood of fragment breakup upon impact. Consequently, the collected fragments could not be used for validation of the imaging results, and are not discussed further here.)

Post-processing of these images to extract fragment size and velocities is achieved in a three-step process implemented in custom MATLAB® algorithms. As is almost always done in image based tracking, the first step is object segmentation from the background. As seen in Fig. 10, fragments appear dark in contrast to the light background. Here we choose to utilize our image segmentation routines originally developed for DIH.[13] Connected dark regions are selected based on an optimum threshold which maximizes the edge sharpness, defined as the mean absolute value of the Sobel gradients for the pixels along the region boundary. For example, the colored outlines in the bottom row of Fig. 10 show object boundaries selected with this technique. By selecting local optimum thresholds, the current segmentation technique is robust against fluctuations in the background intensity, which are commonly caused by flash and smoke in explosive operations. Still, the literature contains many alternative segmentation techniques and a complete study has yet to be conducted to identify the optimum technique.

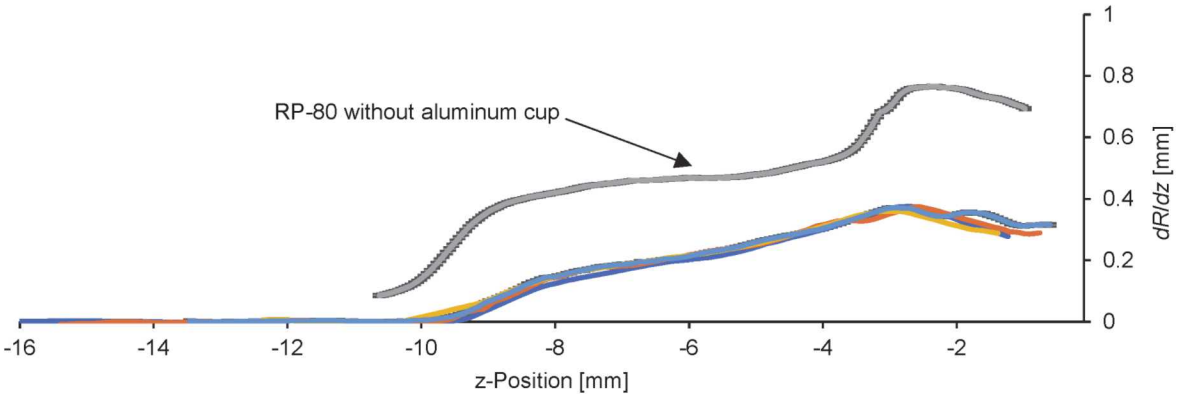

Fig. 9. DIC profiles of the change in radius, *dR*, at a select time point for five tests. 1σ error bars shown are typical of all tests with an average estimated error of ± 4.8 μm.

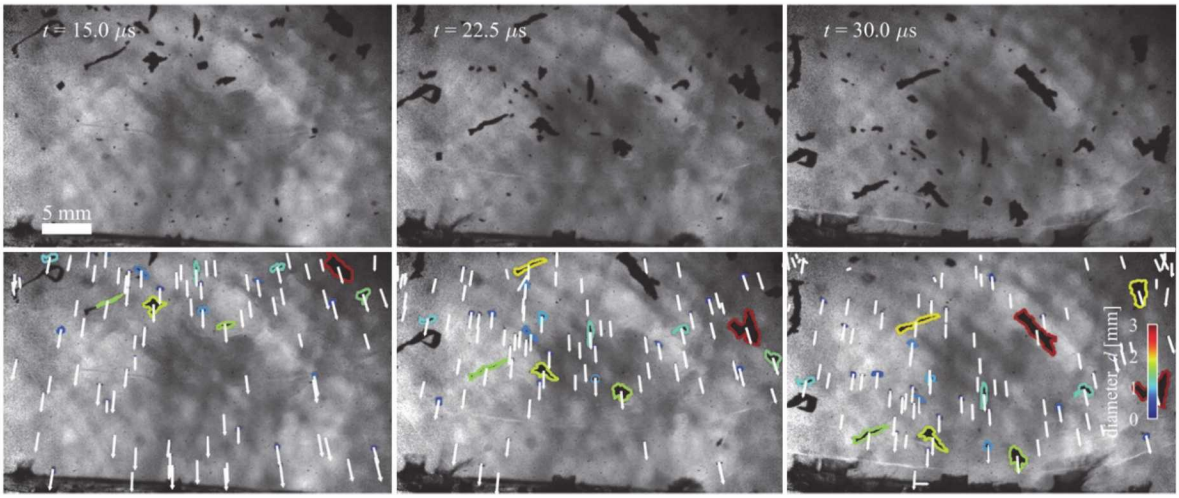

Fig. 10. (top) Raw images showing fragments from an RP-80 detonator recorded at 2 MHz. (bottom) Measured 2D fragment trajectories at three select frames.

Following segmentation, temporal fragment tracking is needed to connect identical fragments between frames. Here, the use of a stereo camera configuration ensures that temporally resolved 3D trajectories can ultimately be measured. Multiple processing techniques could be considered. A direct 3D tracking method would first select matching fragments between the left and right camera, triangulate their 3D position, and then find temporal trajectories by connecting the most likely 3D neighbors from one frame to the next. Alternatively, the object regions could first be tracked in 2D by independently processing each video, followed by 3D triangulation of matching 2D trajectories. This is the method chosen here. We believe this has many advantages for tracking of explosively generated fragments. For example, as shown in Fig. 10, fragment shapes are highly non-spherical, and the true center of mass cannot be accurately measured in each 2D image. With relatively narrow stereo angles, the uncertainty of the triangulated out-of-plane position is already inherently high. When this is compounded with the relatively inaccurate 2D centroids, the result is significant scatter in the frame-to-frame triangulated depth positions. This can make temporal matching of individual 3D fragment positions very difficult. In contrast, as shown in Fig. 10, in the 2D videos, fragments tend to follow straight paths which can be robustly located with automated routines. Assuming acceleration is insignificant over the chosen FOVs, measured 2D trajectories can be fit to constant velocity models, which helps to reduce the effect of frame-to-frame uncertainty in the 2D centroids before 3D triangulation.

Once again, the literature contains many potential methods for tracking fragments in the 2D videos with extensive work conducted by the community focused on Particle Tracking Velocimetry (PTV).[14] Here, we again leverage our tracking techniques originally developed for video rate DIH[15], which are themselves from ideas proposed by the PTV community.[16] In this method, initial estimates of matching 2D trajectories are fit to linear models with respect to time. These models are then extrapolated over a fixed number of frames to locate and stitch together multiple trajectories and add regions which have not yet been assigned to a trajectory. Initial estimates which do not lead to trajectories of sufficient temporal length are discarded, and the process is iterated. When completely successful, this method connects individual fragments into complete trajectories such that every fragment is measured as one and only one trajectory, eliminating potential biases.[17]

The choice of initial guesses is critical to ensure the 2D tracking converges quickly and accurately. Previously, we used nearest-neighbor matching to find these initial trajectories.[15] However, due to the extreme velocities in the current experiment, fragments may move a significant distance from one frame to the next, such that

nearest-neighbor matching is susceptible to false linking. To address this, we instead use an initial three-frame matching routine which selects initial trajectory estimates as those with the minimum average acceleration between the three frames. We find this to be particularly robust for the current application due to the comparatively small accelerations and linear trajectories expected through the small FOVs.

The bottom row of Fig. 10 shows the 2D fragment trajectories measured with this technique. Here the arrows show the measured velocities while the outline colors correspond to the area equivalent diameter assuming constant image magnification through the measurement volume.

Fig. 10 results correspond to the left camera. Results from a second stereo camera, synchronized to the left camera, are processed in a similar manner. This results in 2D fragment trajectories through two FOVs separated by roughly 30°. In the final step in the process, 3D resolution is obtained by triangulating the 2D trajectories. For this, the smoothed in-plane positions predicted by the linear fit to the measured positions are triangulated on a frame-to-frame basis for every potential trajectory match. The best matches are selected from those which have a minimum average triangulation error. This is defined as the average of the epipolar triangulation error for every frame containing a measured fragment in both the left and right cameras.

For a range of different fragmenting explosives tested, we have found this three-step technique is capable of accurately tracking a large majority of the fragments visible in both cameras. However, measurements can also be susceptible to noise caused by shock-waves, soot clouds, and image regions with non-ideal lighting. When possible, we find that the resulting false 3D trajectories can be significantly reduced by eliminating as invalid any trajectory which does not linearly extrapolate in time back to the approximate 3D initial location of the explosive device. For example, in the results considered here the RP-80 detonator was placed ~75 mm above the FOV and fired 56 μs before the start of recording. Therefore, the 3D trajectories in this work were linearly extrapolated to -56 μs. Final trajectories were only accepted when the predicted 3D position was within a small radius of the initial detonator location.

Fig. 11 shows the triangulated 3D trajectories at a select instant in time. The top row shows the recorded left and right frames while the bottom row shows the triangulated fragment depths, *z*-location, along the horizontal axis plotted against the triangulated fragment height, *y*-location, on the vertical axis. Mean area equivalent fragment diameters are shown with colors. Here, the diameters are found from the effective magnification at the triangulated depth. Notice that the largest fragments are confined to a narrow optical depth in the bottom plot. This matches the behavior in Fig. 5, where the large fragments from breakup of the cylindrical portion of the detonator are observed in a tight ring.

Work is ongoing to quantify the uncertainty of these measurements. Velocity uncertainty has been initially estimated with a Monte Carlo approach that dithers the measured particle centroids and retriangulates the 3D positions. Assuming one-pixel centroid uncertainty, the standard deviation of velocity uncertainty is estimated to be ~10 m/s in the in-plane, *x*- and *y*-directions, and ~70 m/s in the depth, *z*-direction. This is equivalent to 1% and 8% in the in-plane and depth-directions, respectively, compared to the average total fragment velocity of 890 m/s.

Accuracy of the measured sizes is more difficult to assess. Due to the highly non-spherical nature of these fragments, measures of fragment volume or mass are expected to be less accurate compared to measures of the in-plane morphology. Because accurate fragment mass is crucial for determination of impact kinetic energy and momentum, more work dedicated to quantifying and improving this uncertainty is particularly warranted.

The techniques introduced in this and the previous sub-section allow for detailed quantification of explosive fragmentation beginning with case strain and ending with a polydisperse distribution of fragment sizes and velocities. At the length-scales presented here, experiments are cost effective and relatively easy to reproduce. Ongoing work focuses on repeating and processing many such experiments such that the statistical nature of detonator fragmentation can be quantified and measurement uncertainty can be estimated.

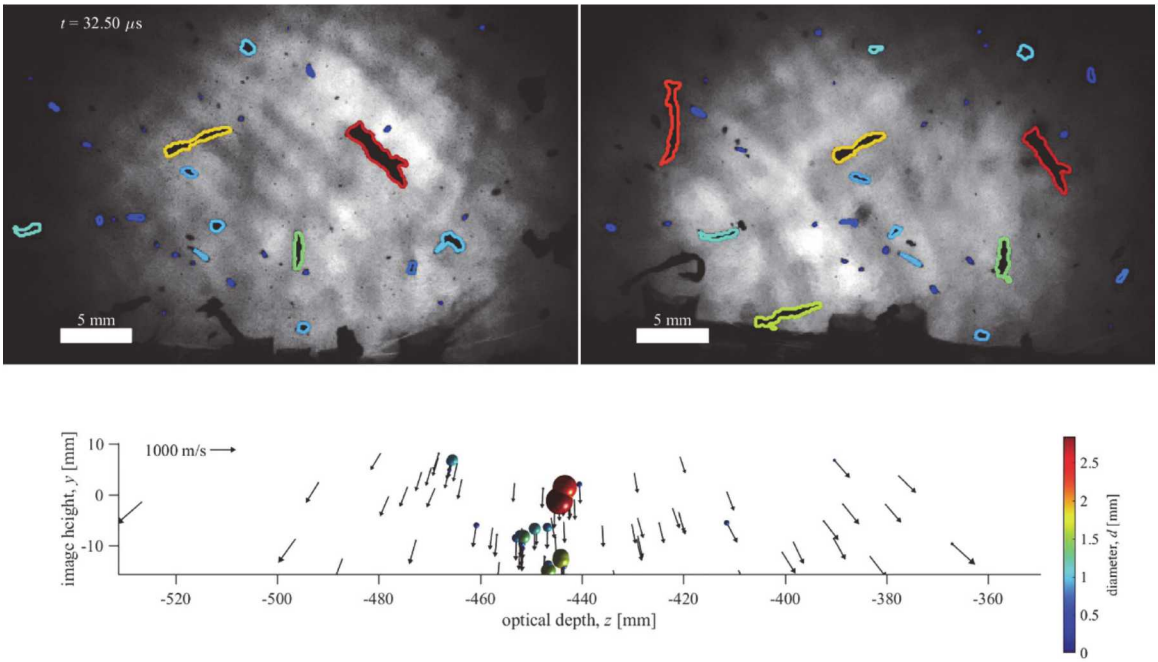

Fig. 11. Triangulated 3D fragment trajectories. (top) Left and right camera images overlaid with the measured fragment outlines at one instant. (bottom) The corresponding triangulated velocities.

Fragment Impact Experiments

Finally, this section demonstrates initial work to apply these techniques for investigation of fragment impact and initiation. Once again, we utilize the generic aluminum capped detonators discussed in Yeager *et al.*[5]

The DIH configuration shown in Fig. 2 has been integrated with sufficient hardware protection to allow fragment measurements simultaneous with PBX impact and initiation. Fig. 12 shows initial results. The left shows a raw hologram image while the right has been numerically refocused to the approximate optical depth of the PBX pellet. As was the case in Fig. 3, DIH is again able to resolve the first fragments. Yet again, however, downstream fragments are obscured by leading shockwaves. Therefore, without the phase-conjugate methods shown in Fig. 4, DIH remains difficult at the go/no-go transition where multiple fragment impacts and shock-convergence could lead to initiation.

Video tracking using a single camera was performed simultaneous with the DIH shown in Fig. 12. Results are shown in Fig. 13. This illustrates an interesting test case where two fragments impact the pellet. The first impact, which does not lead to initiation, has a measured impact velocity of 2.72 km/s and is estimated to have a diameter of 530 μm and 125 μm thickness. The second, which does lead to initiation, has a measured impact velocity of 2.40 km/s and is estimated to have a diameter of 750 μm and 125 μm thickness.

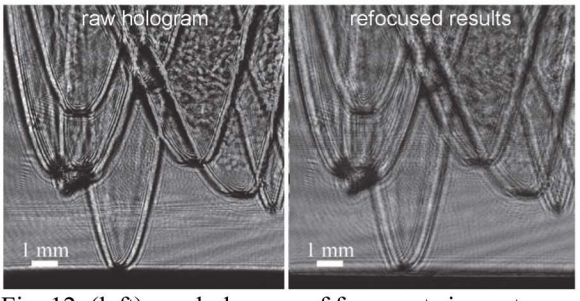

Fig. 12. (left) raw hologram of fragments impacting PBX 9407 leading to initiation, (right) results after numerically refocusing. Fragments travel from top to bottom.

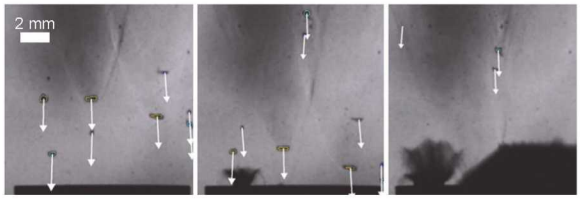

Fig. 13. Video results of fragments impacting PBX 9407.

Fig. 13 results provide clear video evidence of a go/no-go transition and will serve as a useful sanity check for modelers. However, we are ultimately interested in the possibility of multiple fragment impact leading to increased likelihood of initiation. For that, we have very recently started experiments using the stereo fragment tracking methods to study the detailed 3D distribution of the size, velocity, and shapes of fragments leading to impact. An initial result showing clear initiation is shown in Fig. 14.

Conclusions

This work presents experimental methods to study fragmentation of metal case explosives at the detonator scale (dimensions on the order of tens of mm and explosive weight on the order of grams). Digital Image Correlation (DIC) using 5 MHz cameras provides 3D spatial and temporal resolution of the case strain leading to fragmentation. Digital Inline Holography (DIH) provides 3D resolution of fragment flight using a single camera, but is susceptible to degradation due to shock-waves. This is addressed with proposed stereo fragment tracking methods recorded at 2 MHz. Demonstrated techniques enable temporal resolution of the size and 3D trajectory of each fragment. Finally, initial attempts to apply these techniques to study fragment impact on PBX pellets are presented.

Future work focuses on resolving fragmentation statistics for the purposes of model validation. Furthermore, current techniques still cannot resolve the detailed effects of multiple-fragment impact and shock convergence within the PBX that might lead to earlier onset of initiation compared to single-fragment impact. Flash x-ray might provide sufficient contrast and is currently being explored. However, timing and triggering to capture the likely sub-μs dynamics is challenging, and significant work or new ideas are needed.

Fig. 14. Multiple fragment impact leading to initiation of PBX 9407.

Acknowledgments

We greatly acknowledge J. Patrick Ball and Thomas W. Grasser of Sandia National Laboratories for their assistance with the setup and acquisition of the experimental results shown here. This work was partially supported by the Laboratory Directed Research and Development program at Sandia National Laboratories as well as the Joint DoD/DOE Munitions Program. Sandia National Laboratories is a multi-mission laboratory managed and operated by National Technology and Engineering Solutions of Sandia, a wholly owned subsidiary of Honeywell International Inc., for the U.S. Department of Energy's National Nuclear Security Administration under Contract No. DE-NA0003525.

Funding was provided jointly by Nuclear Safety Research and Development (via Paul Peterson) and the Joint Munitions Program (via Thomas Mason). Los Alamos National Laboratory, an affirmative action equal opportunity employer, is operated by Los Alamos National Security, LLC, for the National Nuclear Security Administration of the U.S. Department of Energy under Contract No. DE-AC52-06NA25396.

References

1 Francois, E. G., et al., 2010, "Material properties effects on the Detonation Spreading and Propagation of Diaminoazoxyfurazan (DAAF)," Proc. 14th International Detonation Symposium, Office of Naval Research, pp. 1312-1321.

2 Gibbs, T. R., and Popolato, A., 1980, LASL Explosive Property Data, University of California Press, Berkeley.

3 Leininger, L., et al., 2008, "Modeling three-dimensional shock initiation of PBX 9501 in ALE3D," Lawrence Livermore National Laboratory (LLNL), Livermore, CA.

4 Lueck, M., et al., 2011, "Numerical analysis of the initiation of high explosives by interacting

shock waves due to multiple fragment impact," 26th International Symposium on Ballistics, E. Baker, and D. Templeton, eds., DEStech Publications, Inc., Miami, FL, pp. 73-81.

5 Yeager, J. D., et al., 2017, "Characterization of hypervelocity metal fragments for explosive initiation," J. Appl. Phys., 122(035901).

6 Sugawa, S., et al., 2015, "A 20 Mfps global shutter CMOS image sensor with improved sensitivity and power consumption," Proc. Int'l Image Sensor Workshop, pp. 166-169.

7 Cooper, M. A., et al., 2010, "Observations in Explosive Systems with High-Speed Digital Image Correlation," Proc. 14th International Detonation Symposium.

8 Phillip, R., 2012, "Introduction to Digital Image Correlation: Best Practices and Applications," Experimental Techniques, 36(1), pp. 3-4.

9 Sutton, M. A., 2013, "Computer Vision-Based, Noncontacting Deformation Measurements in Mechanics: A Generational Transformation," Applied Mechanics Reviews, 65(5), pp. 050000-050000.

10 Katz, J., and Sheng, J., 2010, "Applications of holography in fluid mechanics and particle dynamics," Annu. Rev. Fluid Mech., 42, pp. 531-555.

11 Guildenbecher, D. R., et al., 2018, "Phase conjugate digital inline holography (PCDIH)," Opt. Lett., 43(4), pp. 803-806.

12 Reu, P., 2015, "Points on Paint," Experimental Techniques, pp. n/a-n/a.

13 Guildenbecher, D. R., et al., 2013, "Digital holography simulations and experiments to quantify the accuracy of 3D particle location and 2D sizing using a proposed hybrid method," Appl. Opt., 52(16), pp. 3790-3801.

14 Dracos, T., 1996, "Particle Tracking Velocimetry (PTV)," Three-Dimensional Velocity and Vorticity Measuring and Image Analysis Techniques: Lecture Notes from the Short Course held in Zürich, Switzerland, 3–6 September 1996, T. Dracos, ed., Springer Netherlands, Dordrecht, pp. 155-160.

15 Guildenbecher, D. R., et al., 2016, "High-speed (20 kHz) digital in-line holography for transient particle tracking and sizing in multiphase flows," Appl. Opt., 55(11), pp. 2892-2903.

16 Li, D., et al., 2008, "A multi-frame particle tracking algorithm robust against input noise," Meas. Sci. Technol., 19(10), p. 105401.

17 Powell, M. S., et al., 2018, "Agglomerate Sizing in Aluminized Propellants Using Digital Inline Holography and Traditional Diagnostics," J. Propul. Power, 34(4), pp. 1002-1014.